

Y-branch optical coupler monolithically integrated with DFB Quantum Cascade lasers.

Alexander Soibel, Kamjou Mansour, Siamak Forouhar,

*Jet Propulsion Laboratory, California Institute of Technology, 4800 Oak Grove Dr, Pasadena, CA 91109
Alexander.Soibel@jpl.nasa.gov*

Milton L. Peabody, Deborah L. Sivco and Alfred Y. Cho

Bell Laboratories, Lucent Technologies, 600 Mountain Ave, Murray Hill, NJ, 07974, USA.

Claire Gmachl

Department of Electrical Engineering, Princeton University, Princeton, NJ, 08544, USA.

Abstract: A Y-branch optical coupler monolithically integrated with two DFB Quantum Cascade Lasers has been demonstrated and studied.

The mid-infrared (mid-IR) spectral range (5 - 20 μm) is of particular interest for optical spectroscopy, remote sensing and infrared countermeasures. Quantum Cascade (QC) lasers, based on intersubband transitions in semiconductor heterostructures,[1] are becoming primary semiconductor optical sources for the mid-IR spectral range. Yet, the output power of these lasers is still too limited for many applications, such as remote sensing and IR countermeasures. One method to increase the total optical power is to combine the emission from several QC lasers by an optical coupler. Moreover, coupled Distributed Feedback (DFB) QC lasers with close emission wavelengths can be used for tunable signal generation at GHz and THz frequencies. The combined output from the two DFB QC lasers will exhibit beating at GHz and THz frequencies ranges, that can be employed for tunable signal generation based on photomixing or sum-frequency-generation.[2]

In this work, we present an experimental realization of a Y-branch coupler that was monolithically integrated with two DFB QC lasers. The Y-branch coupler combines non-coherently the output light from the both lasers. The combined optical signal can be further amplified by applying bias voltage/current to the Y-branch fabricated from QC laser material. DFB QC lasers connected to the Y-branch emit at distinct Bragg wavelengths that are shifted one from another. The wavelength difference between the two lasers causes beating of the output signal at the laser difference frequency that can be varied continuously by the laser bias currents, which tune each laser in wavelength. A difference in the emission wavelengths between the two DFB QC lasers was realized by fabricating lasers that have slightly different width of the waveguide ridge. The ridge width differences in our devices were varied from 0.25 to 1 μm , which resulted in frequency shifts of $\Delta f \sim 10 - 100$ GHz.

Figure 1a shows an optical image of the Y-branch coupled to the two DFB QC lasers. This coupler is based on the laser waveguide structure and is fabricated concurrently with the laser waveguide ridges. The details of the Y-branch shape and dimensions are shown at Fig. 1b. Bending of the Y-branch waveguide results in an optical loss that was kept small by increasing the radius of the curvature R . [3] Bending loss is small if $(R\Delta/\rho) \gg 1$, where $\rho \approx 5$ μm is half-width of the waveguide and $\Delta = (n_{co}^2 - n_{cl}^2)/n_{co}^2 \approx 0.9$ with n_{co} and n_{cl} are refractive indexes of the waveguide core and of the cladding. Low loss requirements is $R \gg 6$ μm that was satisfied in our design with $R = 125$ μm .

QC lasers used in this work are based on "three-well-vertical" transition active regions and were designed for emission at 7.1 μm . The lasers and Y-branch were processed as deep etched ridges with SiN insulating coating that covers the ridge sides, bottoms, but not the ridge tops to allow metallic interconnect between the top contact and the bonding pad. DFB QC lasers were made by etching a first-order grating into the topmost layers of the ridge waveguide. The devices were mounted inside a nitrogen flow cryostat and all measurements were performed at cryogenic temperature ($T = 77$ K) in the pulsed mode. At $T = 77$ K, the resistivity between the Y-branch and the QC laser contact was $r_{\pi} = 70$ Ω , which is much larger than the QC laser differential resistance $r \sim 1$ Ω , and allowed to bias QC lasers and Y-branch independently.

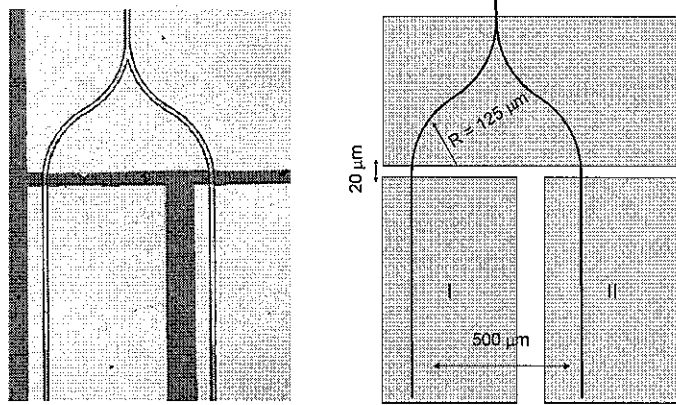


Fig. 1a (left) Optical image of the Y-branch coupler monolithically integrated with two DFB QC lasers; Fig. 1b. (right) Schematic drawing of the device, where QC lasers are marked by I and II.

Light output versus current (L-I) characteristics of lasers I and II operating independently are shown in Fig. 2 by curves 1 and 2. Curve 3 shows the simultaneous operation of both lasers that are connected in parallel to the same current source; in this case only half the current is flowing through each laser. In both measurements, the Y-branch contact was kept floating and no realignments of the laser/detector were performed between the measurements. All output power was measured through the Y-branch output facet. In order to analyze device performance, we add the output powers of both lasers at the corresponding current during the laser independent operation, and we plot the total output power vs. current in one device (curve 1 + curve 2 = curve 4). Since both lasers have almost identical voltage-current characteristics, the current in each laser is half of the total applied current at the simultaneous operations. This allows us to rescale curve 3 to plot the total output at simultaneous operation vs. current in one laser (curve 3, rescaled = curve 5) and to compare curves 4 and 5. Curves 4 and 5 are nearly identical, which demonstrates the efficient operation of the Y-branch. Y branch coupler combines emission from both lasers, thus total power is sum of the each laser output. Further a mplification of f the total output power could be achieved by applying the bias to the Y-branch contact.

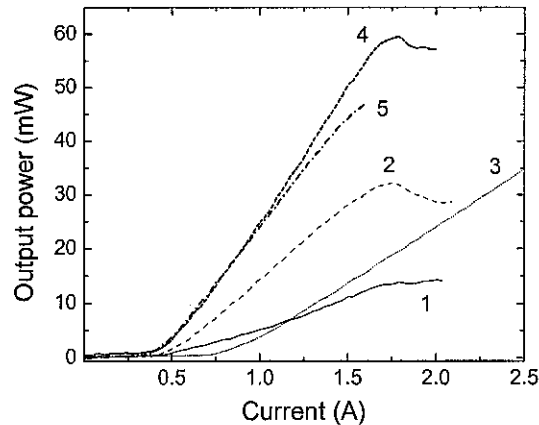


Fig. 2. L-I characteristic of the device operating at 77 K in pulsed mode. Curves correspond to different modes of operation as described in the text.

Optical spectra of lasers I and II operating independently are shown in Fig. 3a and 3b, and optical spectrum of the simultaneous operation is plotted in Fig. 3c. When operated independently, lasers I and II emit single mode at $\lambda_1 \approx 7.03 \mu\text{m}$ and $\lambda_2 \approx 7.04 \mu\text{m}$, where the wavelength shift is caused by small difference in the width of the waveguide ridge. When both lasers are connected and operated simultaneously, the total output spectrum is a sum of the individual spectrum of each laser that demonstrates again the optical combining by the Y-branch. Here, the difference in the laser wavelengths is $\Delta\lambda_1 \approx 0.01 \mu\text{m}$, that gives the beating frequency of the output signal $f \sim 25 \text{ GHz}$.

The research described in this publication was carried out at the Jet Propulsion Laboratory, California Institute of Technology, under a contract with the National Aeronautics and Space Administration.

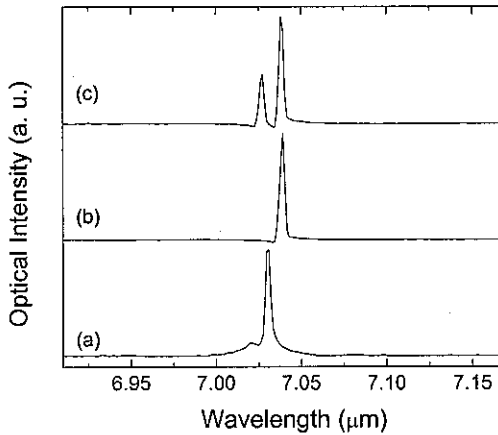


Fig. 3. Optical spectra of laser I (a) and II (b) operating independently and optical spectrum under simultaneous operation of I and II (c).

1. F. Capasso *et al.*, "Quantum Cascade lasers: ultrahigh-speed operation, optical wireless communication, narrow linewidth, and far-infrared emission", *IEEE J. Quantum. Electron.* **38**, 511-532 (2002).
2. E. R. Brown *et al.*, "Photomixing up to 3.8 THz in low-temperature grown GaAs," *Appl. Phys. Lett.* **66**, 285-287 (1995).
3. F. Landouceur and J. D. Love, "Silica-based buried channels waveguide and devices" (Kluwer Academic Publishers), Chap. 10.